

THE ACTIVE ZONE MOBILITY IN A MAGNETIZED DISK WITH ADVECTION

Krasimira Dimitrova Yankova

Space Research and Technology Institute – BAS

Space Astrophysics Department

E-mail: f7@space.bas.bg

**XI BULGARIAN-SERBIAN
ASTRONOMICAL CONFERENCE 2022**



➤ Advective mechanism

➤ Active zone

- Location

- Width

- Separation

- Evolution

Advection

Thermal stability

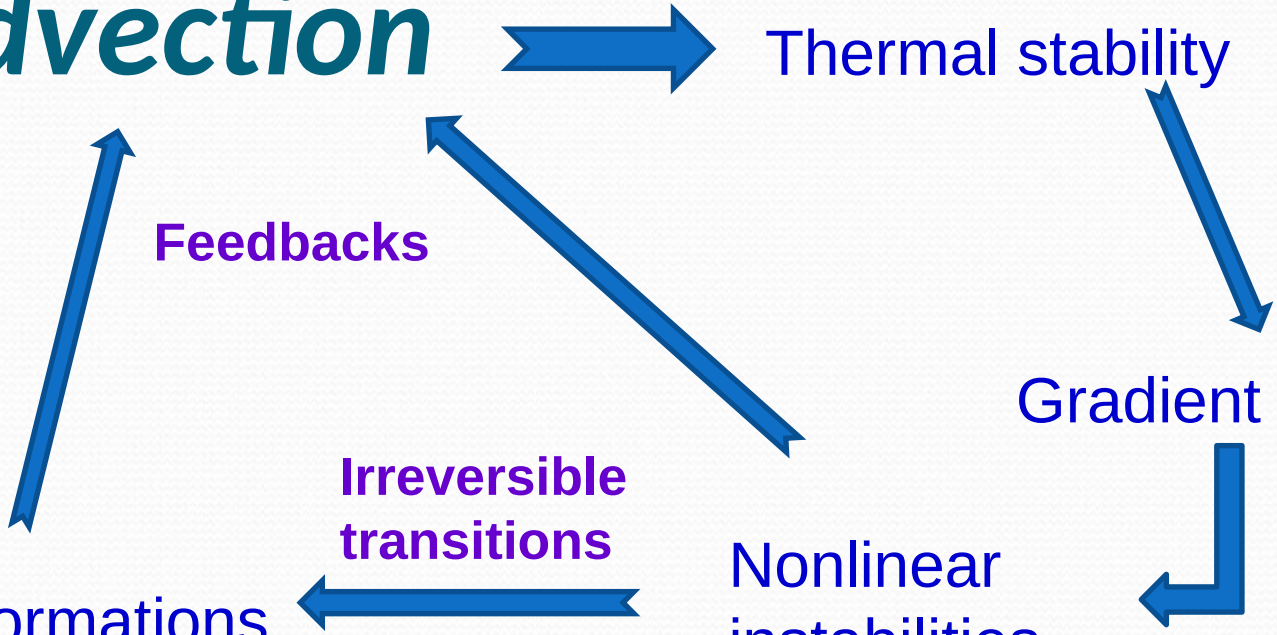
Gradient entropy

Nonlinear instabilities

Irreversible transitions

Feedbacks

Formations



Advective mechanism in $M(n, m-n)$

$$\left(\partial_{t_i} + v_{ij} \partial_{x_j} \right) v_{ji}, \quad \text{where} \quad v_{ij} = \frac{\partial \chi_i}{\partial t_j}$$

and $N(n,0)$

$$\left(\partial_{t_i} + v_{ij} \partial_{x_j} \right) \lambda_{ji} = \beta_{ji} \partial_{t_i} + \delta_{ij} \partial_{t_j}$$

time shifting is a real part of the advective operator

In the case of the disk accretion the advection manages to force more photons to move in orbits for massive particles because they cannot leave the mainstream due to high flow density;

(‘*’)Then the stress tensor for massive and non-massive particles is collective, only with small correction for the leaving photons. This also applies to sum self-gravity flow:

$$\rho_{eq} = \rho_{mater} + \rho_{rad}$$

The active zone is determined by:

- Outer corona radius,

$$-v_s^2 \leq v_a^2 \text{ [lankova 2007a];}$$

-- Inner disk radius, on the first completed by:

$$-K > 1 \text{ [lankova 2009];}$$

$$-\langle v_a \rangle^2 \leq (9/4) \langle v_\phi \rangle^2$$

-- Luminosity distribution by the disk.

The conditions

$v_i^2(x)$

$[x10^6]$

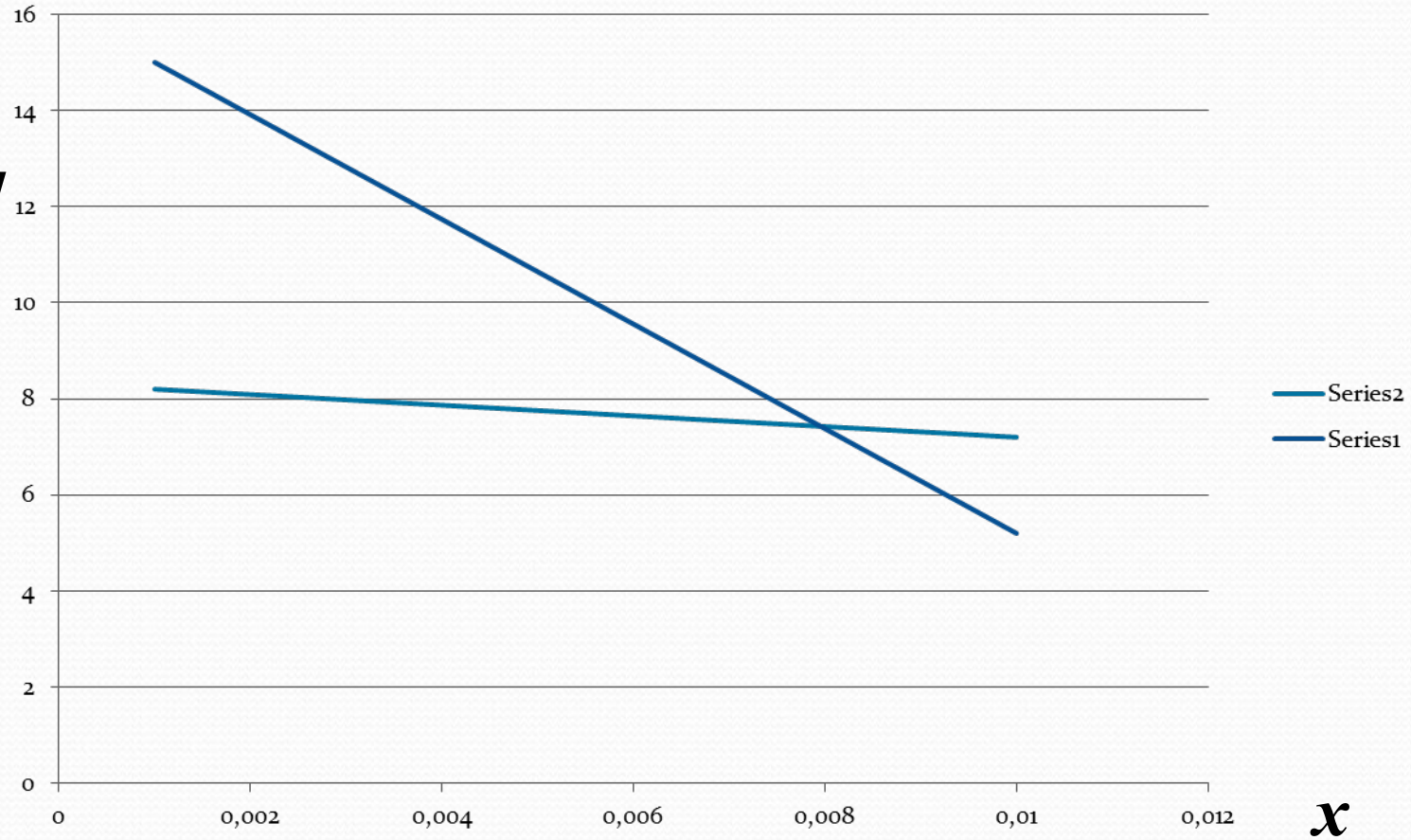


Fig.1a: $\langle v_a \rangle^2 \approx (9/4) \langle v_\phi \rangle^2$

$v_i(t) [x10^6 \text{ cm/s}]$

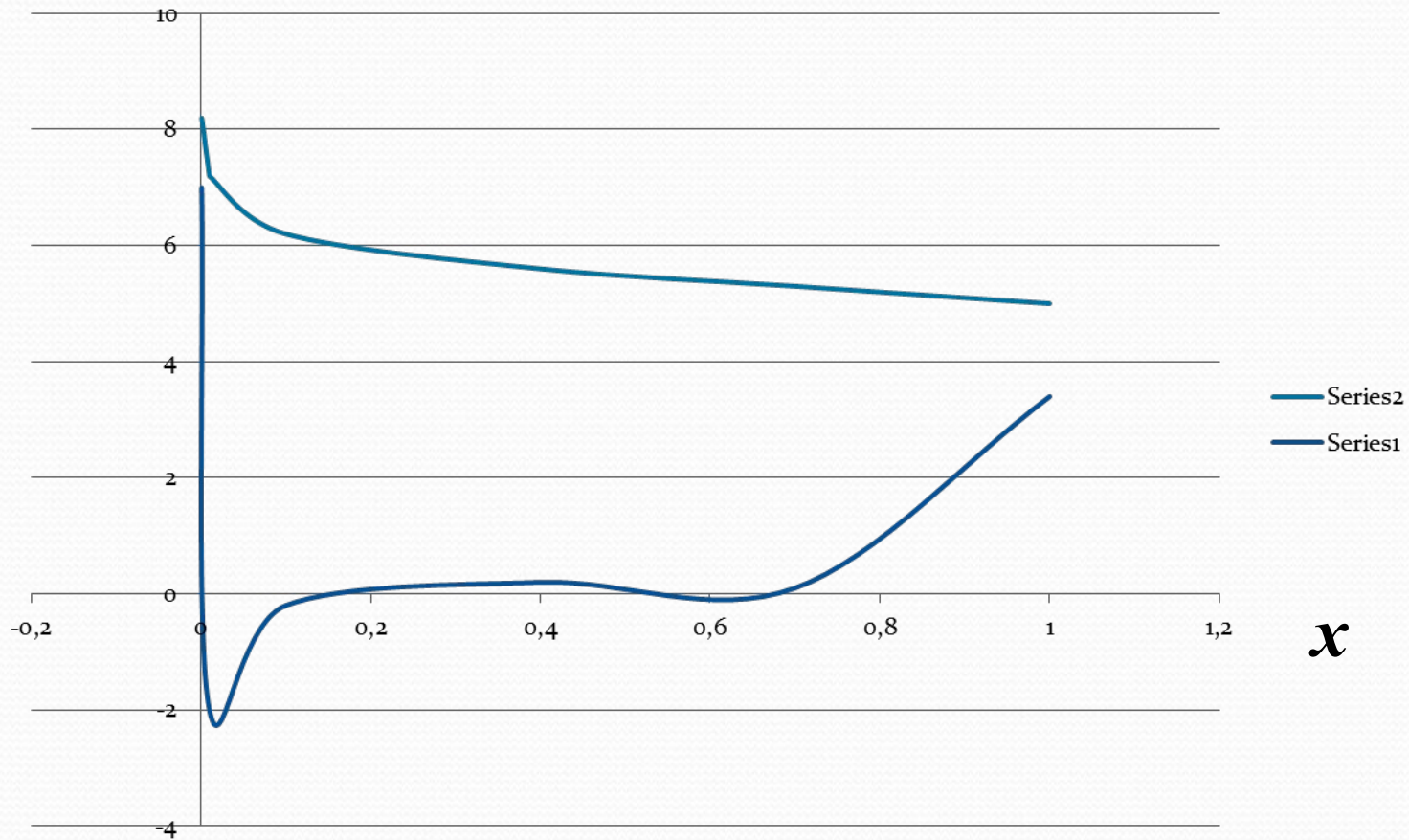


Fig.1b: $\langle v_a \rangle^2 \approx (9/4) \langle v_\phi \rangle^2$

$v_i(t)$ [cm/s]

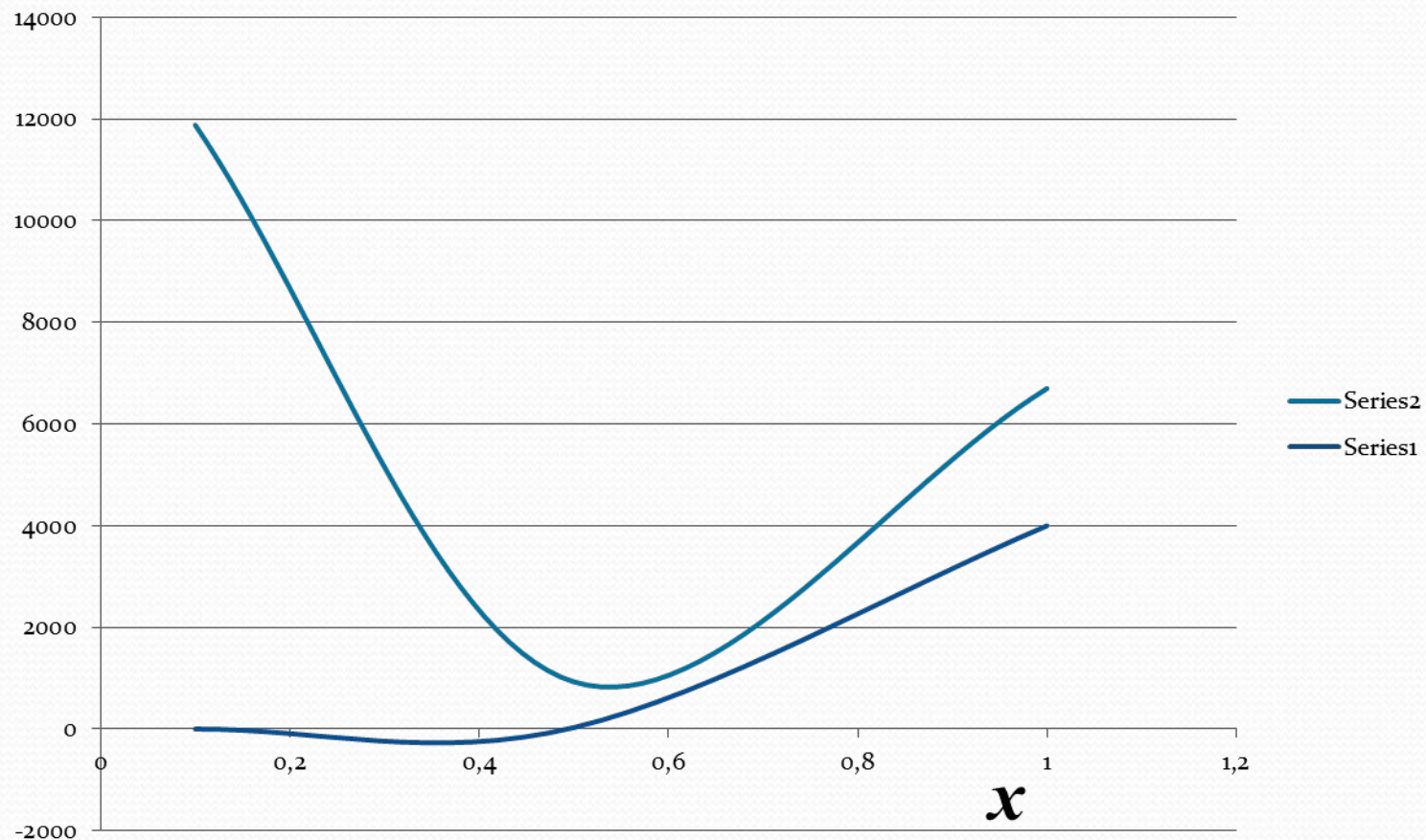


Fig.2: $\langle v_a \rangle^2 \approx \frac{9}{4} \langle v_\phi \rangle^2$

The active zone evolution:

-Outer corona radius, evolution

$$-v_s^2(t) \approx v_a^2(t)$$

-(see Figs.1b-2);

-- inner disk radius, evolution

$$-\langle v_a \rangle^2(t) \approx (9/4) \langle v_\phi \rangle^2(t)$$

-(see Figs.3-4).

$v_i(x) [x10^6 \text{ cm/s}]$

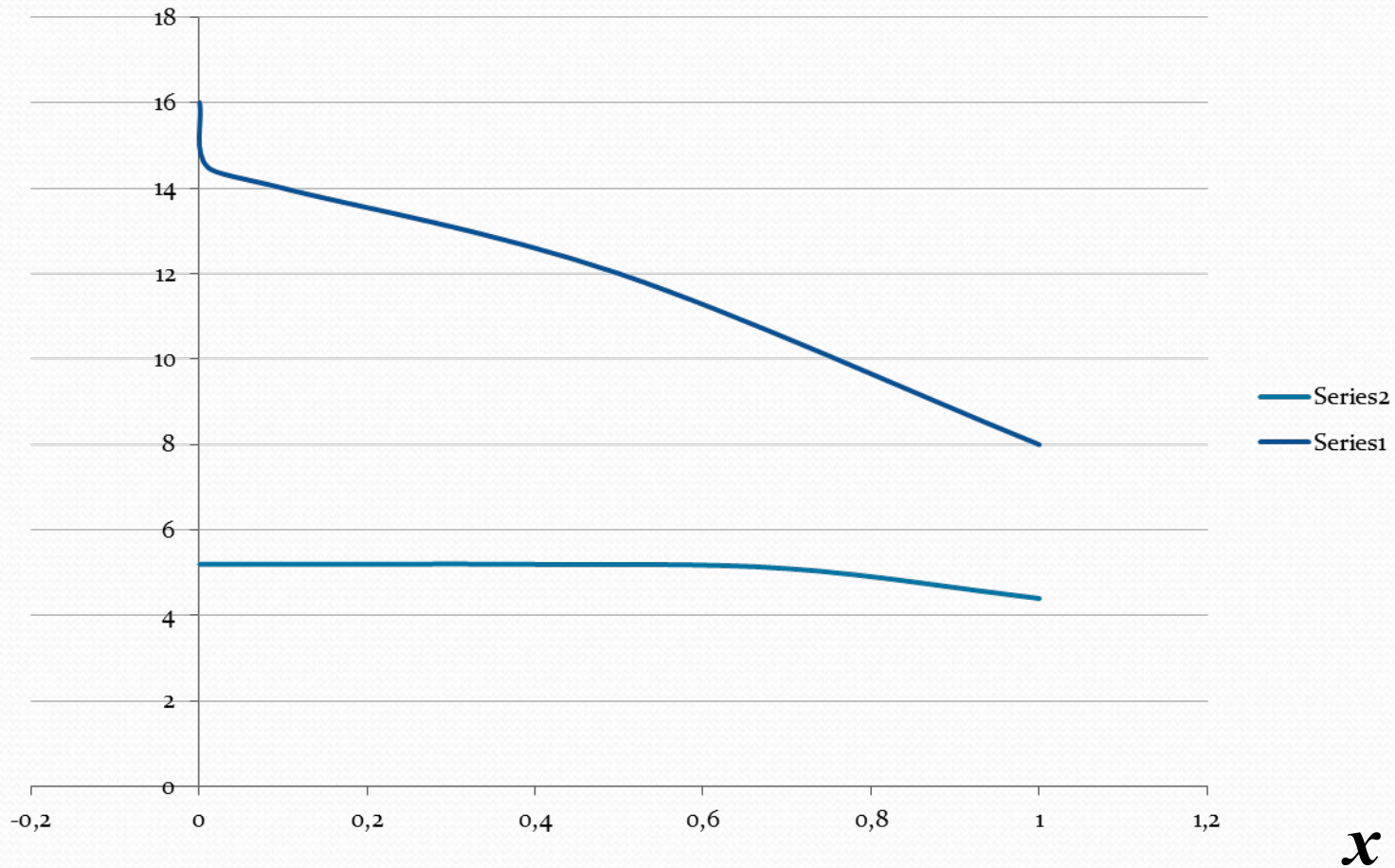


Fig.3a: $|v_s(x)| \approx |v_a(x)|$

$v_i(t) [x10^6 \text{ cm/s}]$

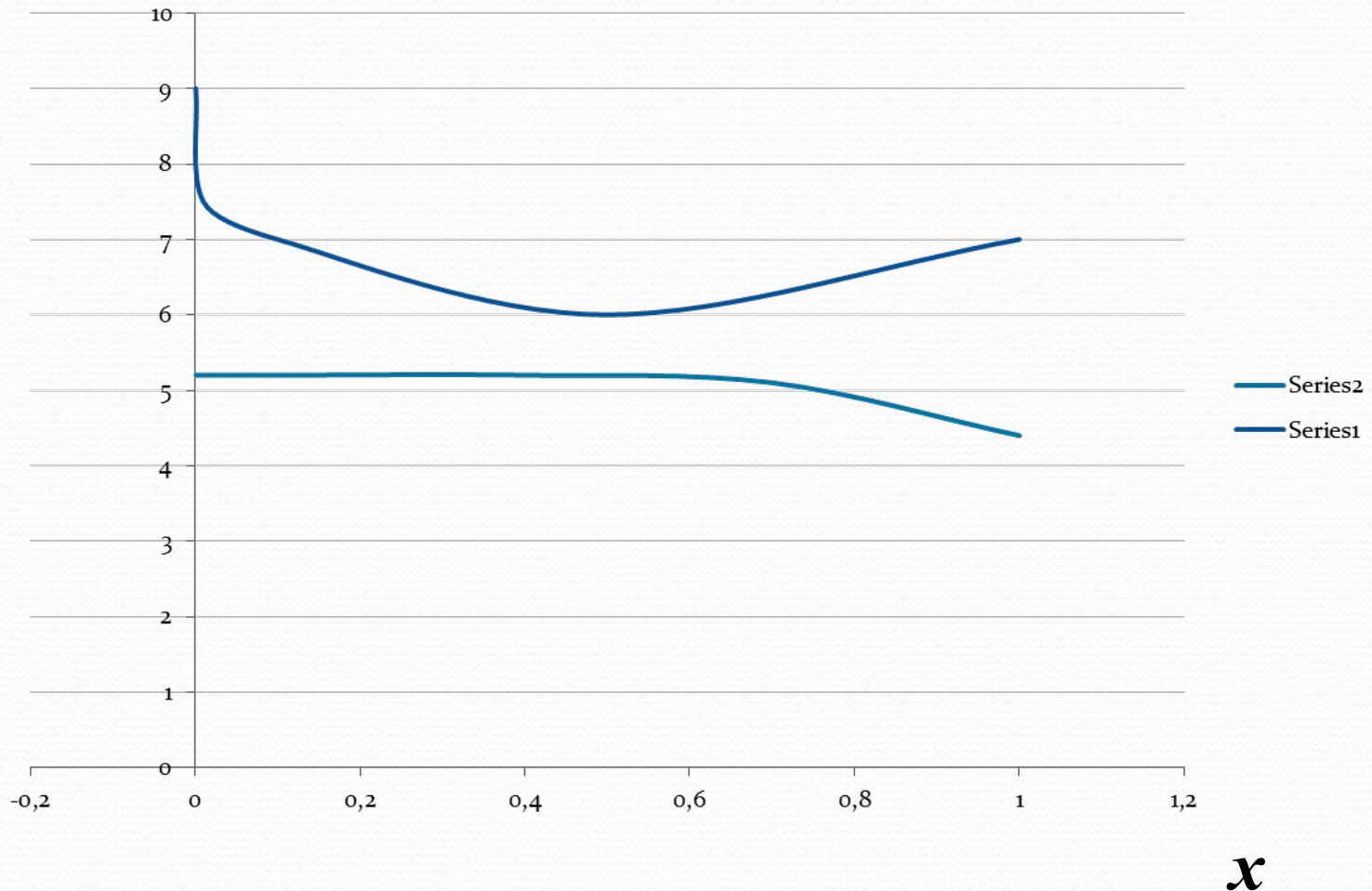


Fig.3b: $|v_s(x)| \approx |v_a(x)|$



$v_i(t)$ [cm/s]

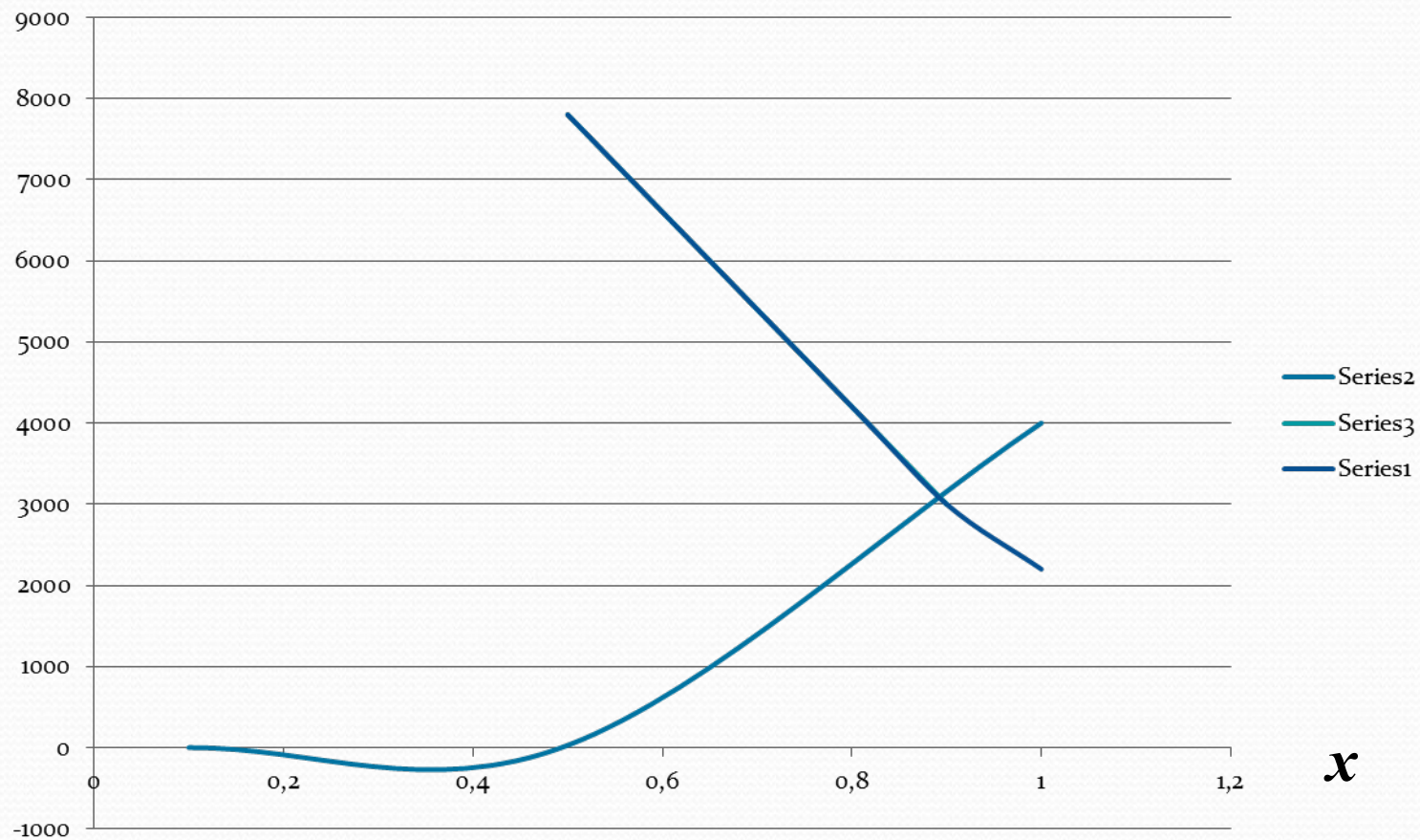


Fig.4b: $|v_s(x)| \approx |v_a(x)|$

Condition $\langle v_a \rangle^2 \approx (9/4) \langle v_\phi \rangle^2$ gives a destruction radius in the range $(0.007; 0.01)R_0$ with a graphic error 10% (see fig.1a) for RS Oph and at $0.1R_0$ for Cyg X-1 (Yankova 2013).

Condition $\langle v_a \rangle^2 \approx \langle v_s \rangle^2$ gives a outer radius of the coronas

at $\sim 340R_g$, for Cyg X-1 (Yankova 2007), (see fig.4a);

at $\sim 45R^*$, for RS Oph ((Yankova 2019), or no corona for RS Oph (see fig.3a)

Log K(x)

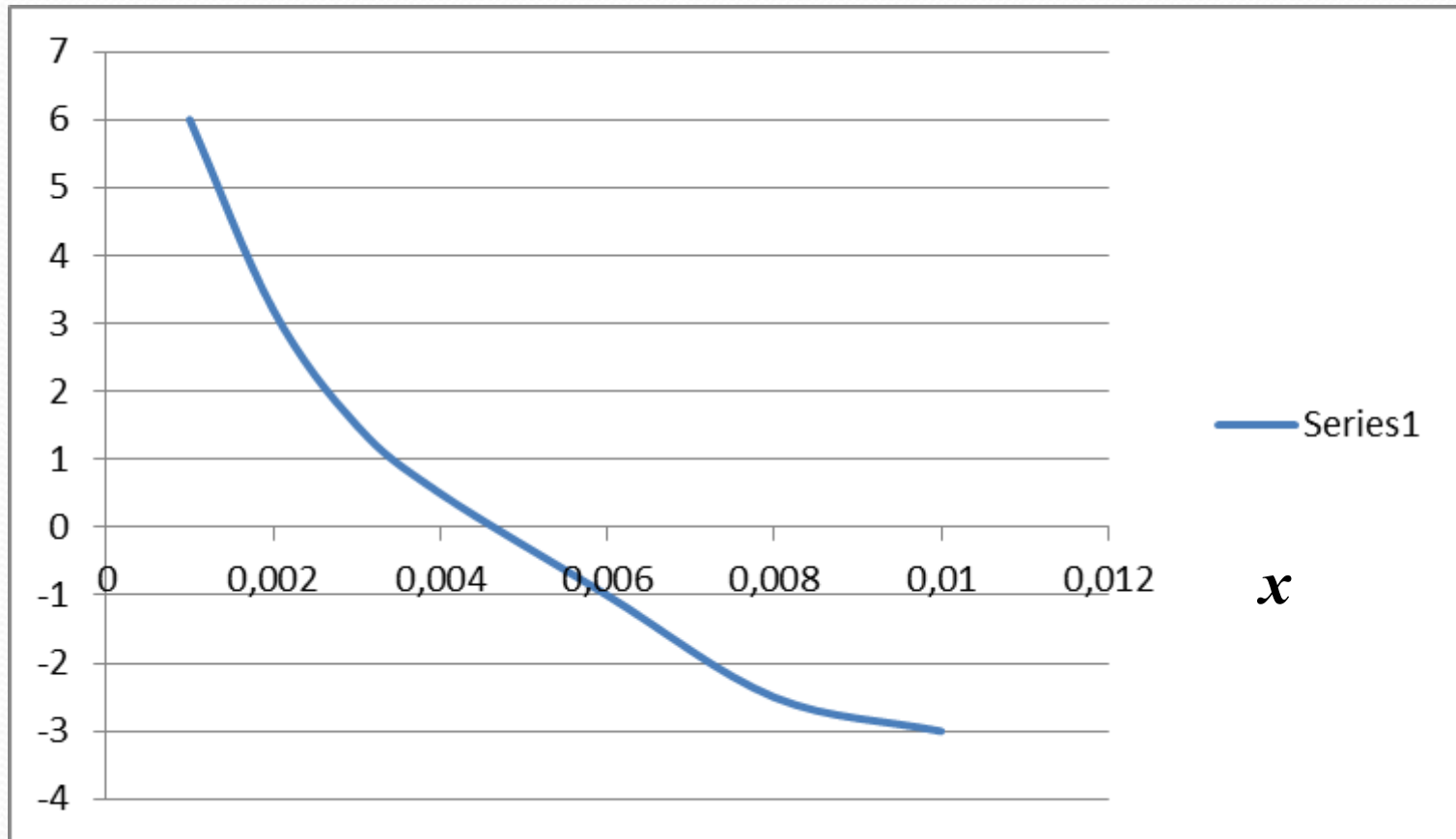


Fig.5: Distribution of the local heating in the RS Oph disk.

Log K(x)

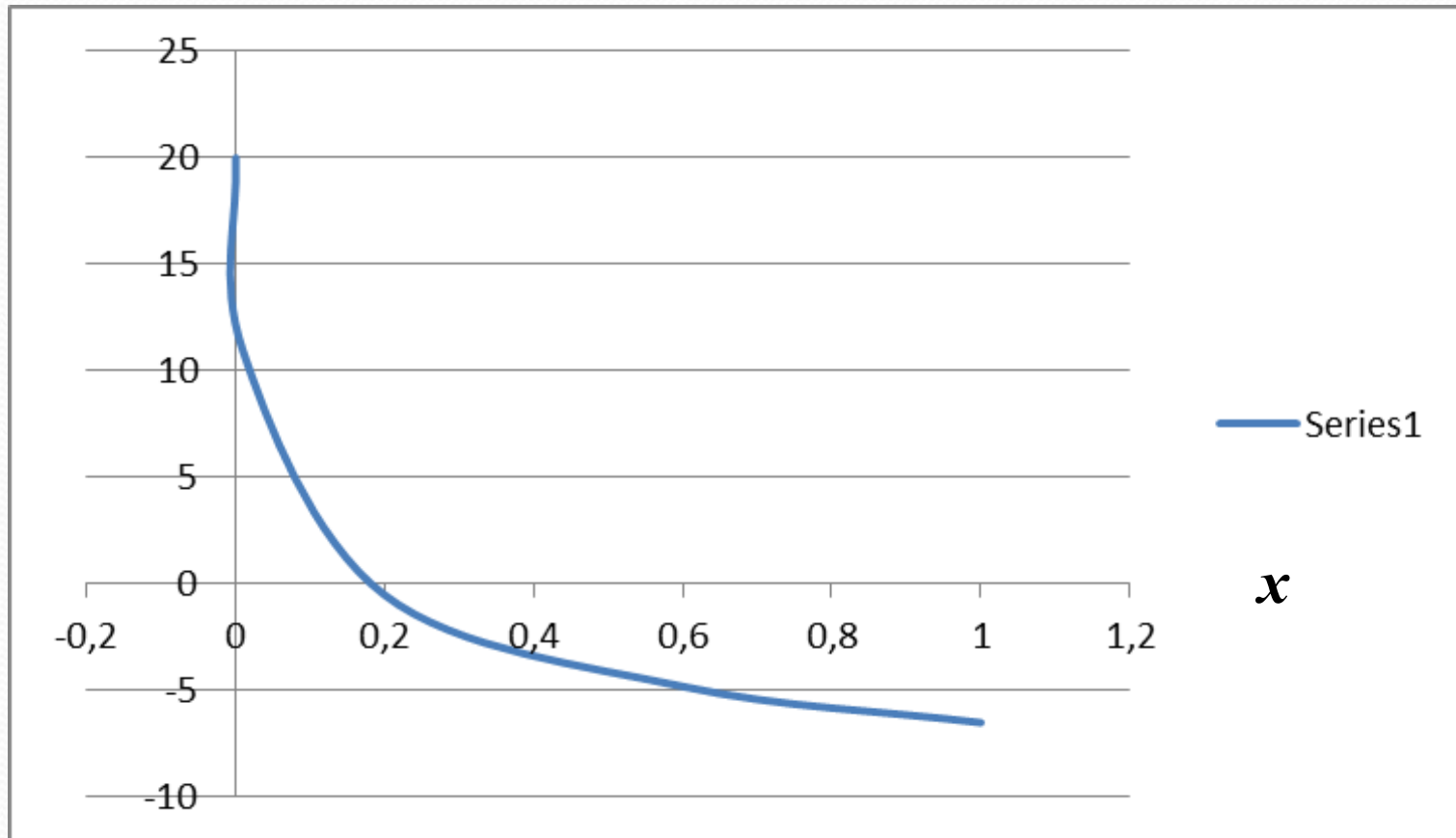


Fig.6: Distribution of the local heating in the *Cyg X-1* disk.

Log L (x)

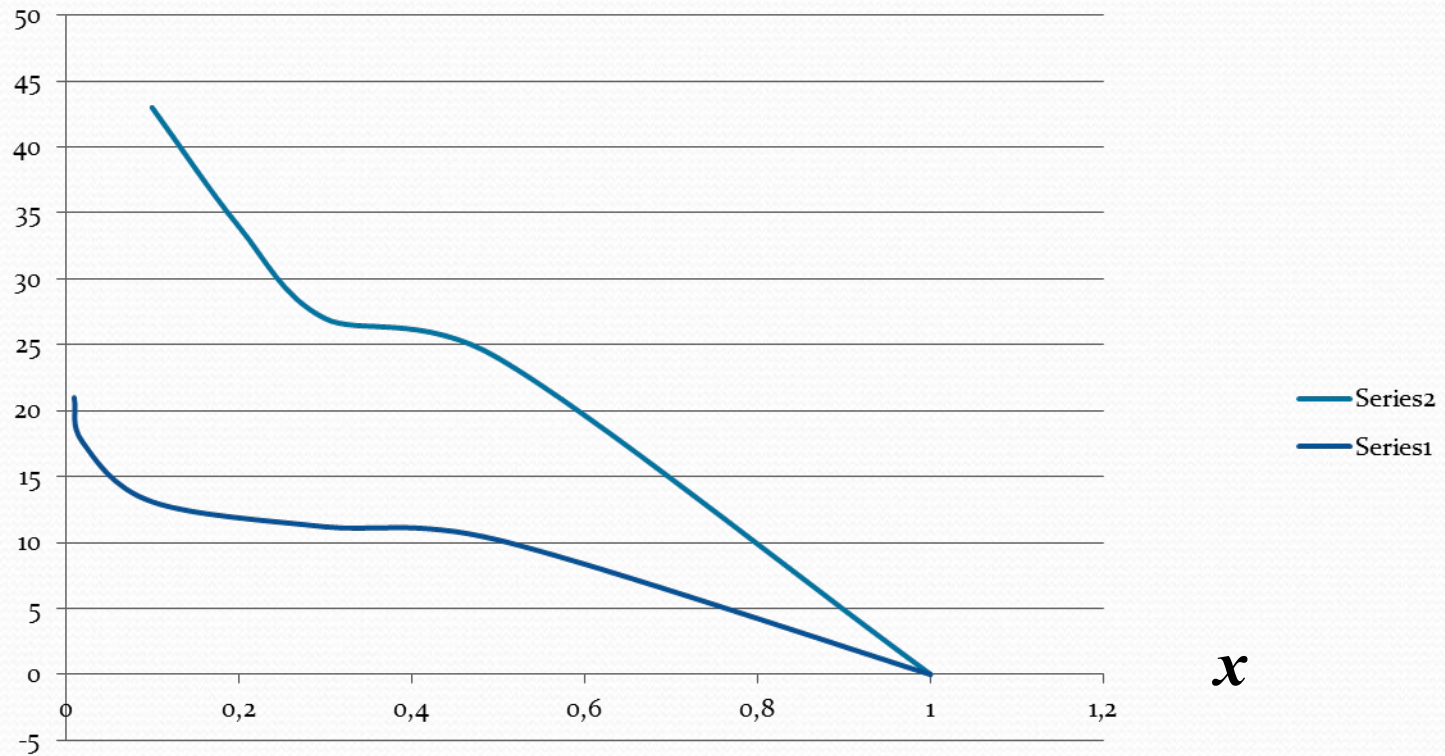


Fig.7: Luminosity distribution function of the RS Oph disk, in two moments.

Log L (x)

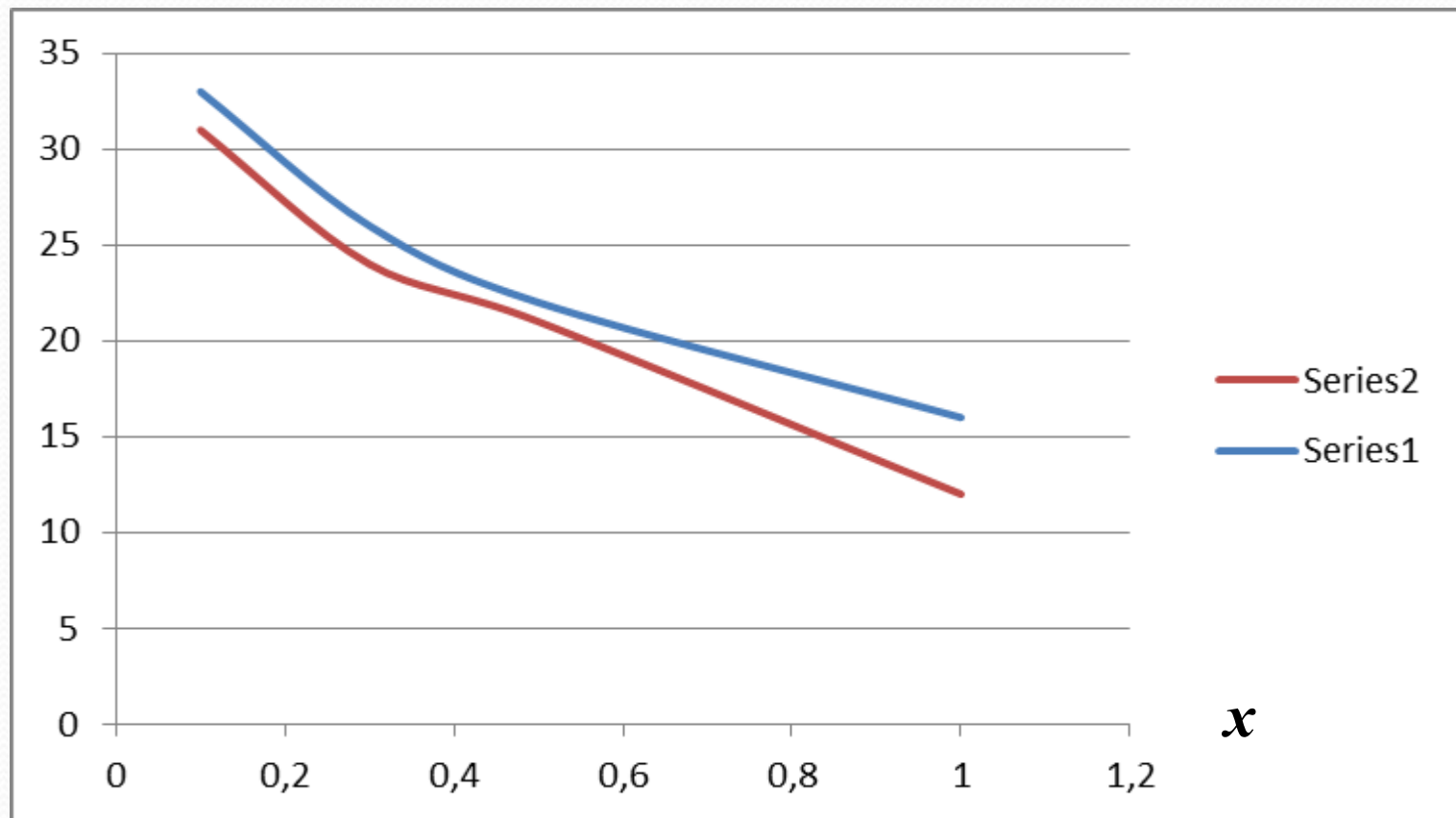
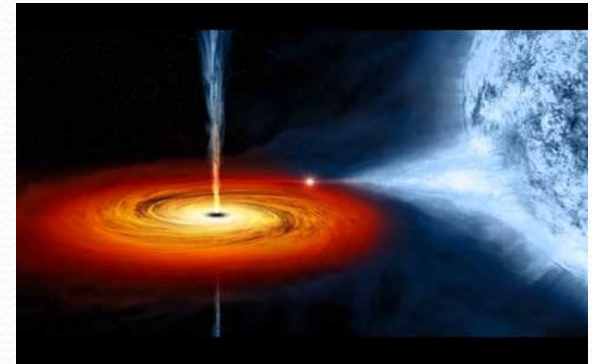


Fig.8: Luminosity distribution function of the *Cyg X-1* disk, in two moments.

We received active zones

in $\sim(0,1;0,4)R_o$, for Cyg X-1,
inner $\sim(0,1;0,2)R_o$; (see *fig.6*)
outer $\sim(0,2;0,4)R_o$



in $\sim(0,007;0,5)R_o$, for RS Oph .
(see *fig.7*)
inner $\sim(0,007;0,01)R_o$;
outer $\sim(0,01;0,5)R_o$



Condition $\langle v_a \rangle^2 \approx (9/4) \langle v_\phi \rangle^2$ gives a destruction radius in the range $0.005R_0$ with a graphic error 10% (see fig.5) for RS Oph and at $0.00?R_0$ (see fig.2) for Cyg X-1.

Condition $\langle v_a \rangle^2 \approx \langle v_s \rangle^2$ gives a outer radius of the coronas

at $\sim 900R_g$, for Cyg X-1 , (see fig.4b);

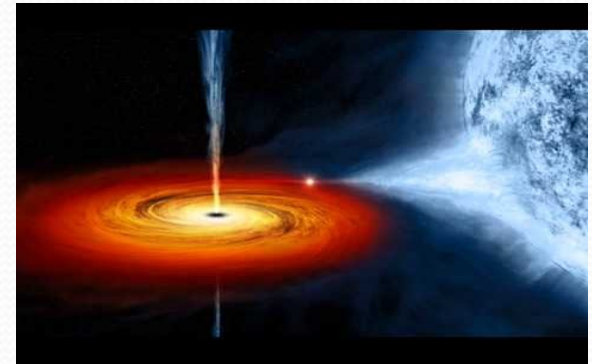
at $\sim 50R^*$, for RS Oph ((Yankova 2019), or no corona for RS Oph (see fig.3b)

We received active zones period later:

in $\sim(0,9)R_o$, for Cyg X-1,

inner $\sim(0,2)R_o$;

outer $\sim(0,9)R_o$



in $\sim(0,005;0,5)R_o$, for RS Oph .

(see *figs.5,7*)

inner $\sim(0,005;0,3)R_o$;

outer $\sim(0,3;0,5)R_o$



We obtained the active zones for the two studied objects at two different moments separated by several evolutionary periods:

Active zone is separated on two parts:

- ✓ Plateau in the Luminosities (see Figs.7-8) indicate the outer active zone in which the advection conceals the activity.
- ✓ In the inner active zone the activity becomes observable [*Yankova, 2019*].

Thank you for your attention

